Proceedings of the 11th ICPMG 2026
11th International Conference on Physical Modelling in Geotechnics
8-12 June 2026, Zurich, Switzerland

Miniature cone penetration testing on a silica sand

R. Ganguly
SLR Consulting, Toronto, Canada, rganguly@slrconsulting.com

A. Sadrekarimi
Western University, London, Ontario, Canada, asadrek@uwo.ca

ABSTRACT: This study evaluates the performance of a reduced-scale Miniature Cone Penetration Testing (MCPT) system for characterizing a silica sand within a controlled calibration chamber designed to replicate in-situ stress conditions. Reconstituted Boler sand specimens were anisotropically consolidated across a range of effective stresses and relative densities to measure cone tip resistance (q_c) and sleeve friction (f_s). The upgraded MCPT apparatus at Western University was optimized for high-precision data acquisition, mitigating scale and boundary effects. Results demonstrate strong correlations between q_c, f_s and key geotechnical parameters including unit weight, relative density, and modulus. The MCPT system consistently reproduced field-like responses and delivered realistic outcomes from loose to dense states. The findings establish MCPT as a cost-effective and efficient alternative to conventional CPT for laboratory studies of silica sands and provide empirical relationships to improve pre-design analyses for applications such as foundation design and soil–structure interaction. The work also underscores MCPT's value for physical modelling programmes by offering a scalable, adaptable approach that bridges laboratory testing and field performance.

1 INTRODUCTION

Cone penetration testing (CPT) is a widely adopted in-situ method for profiling cohesionless soils and assessing their mechanical state. While field CPTs provide valuable continuous data, they are costly and offer limited control over stress history and density. Laboratory-scale Miniature Cone Penetration Testing (MCPT) systems provide a complementary approach, enabling systematic parametric studies under controlled boundary conditions. The upgraded MCPT facility at Western University (Damavandi-Monfared and Sadrekarimi, 2015; Sadrekarimi and Jones, 2022; Ganguly 2019) allows anisotropic consolidation, precise rate control, and high-resolution force measurement. This paper presents an experimental programme on a silica sand conducted using this facility, focusing on cone tip resistance, sleeve friction, and their empirical correlations with unit weight, relative density, and constrained modulus. The goal is to demonstrate the MCPT's capacity to replicate field-like conditions and derive reliable empirical correlations for sand characterization.

2 MATERIALS AND METHODS

2.1 Calibration chamber and instrumentation

The MCPT apparatus in Figure 1 consists of a triaxial-type pressure vessel (≈ 140 mm internal diameter, 130 mm height) fitted with drainage ports and a penetration opening. Because of the flexible membrane, a constant stress boundary condition (BC1) is produced during cone penetration. A 6 mm-diameter, 60° cone with an independent friction sleeve is mounted on an internal load cell assembly capable of resolving < 0.01 N. A servo actuator drives the cone at constant velocity while cell and back pressures are maintained through electronic regulators. The chamber can accommodate isotropic and anisotropic (K_0) consolidation, monitored through vertical and lateral pressure sensors.

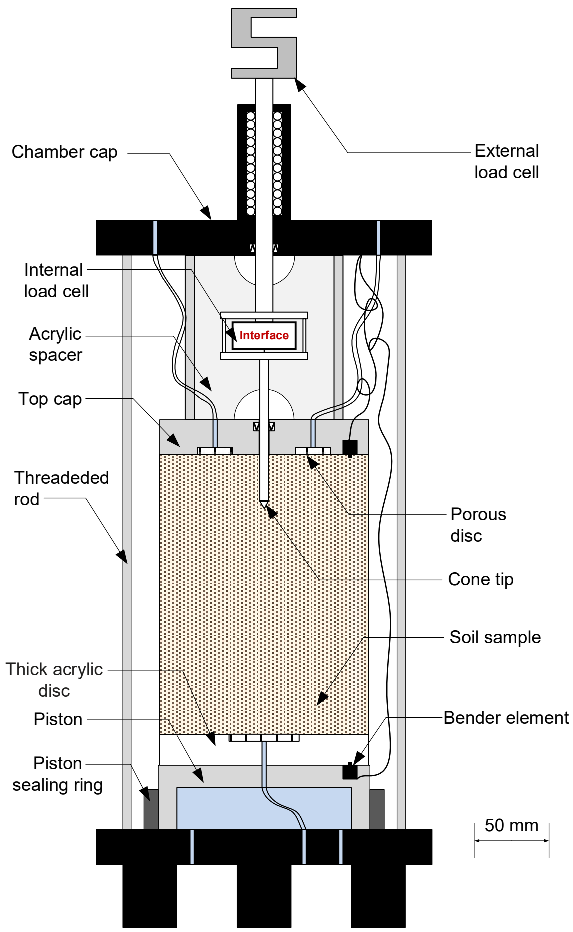

Figure 1. Schematic of MCPT calibration chamber and cone assembly. A scale bar is included to indicate the overall dimensions of the apparatus.

2.2 Tested material

The tested soil was a clean, quartz-rich silica sand, collected from the Boler Mountain (London, Ontario). Its key index properties include specific gravity of particles (G_S) of 2.67, and minimum (e_{min}) and maximum (e_{max}) void ratios of respectively 0.48 and 0.78, all measured following ASTM standard procedures (ASTM 2010, 2014, 2016a, 2016b). According to Figure 2, the tested silica sand had a relatively uniform gradation with a median particle diameter (D_{50}) of 0.24 mm, and coefficients of uniformity (C_U) and curvature (C_C) of respectively, 1.75 and 0.91. As shown in the inset image of Figure 2, the sand particles were subrounded to subangular. Specimens were prepared by air pluviation to achieve average relative densities (D_{rc}) of 27%, 47%, and 65%. After assembly, each sample was saturated using CO_2 flushing and de-aired water percolation, achieving a Skempton's B-value > 0.95.

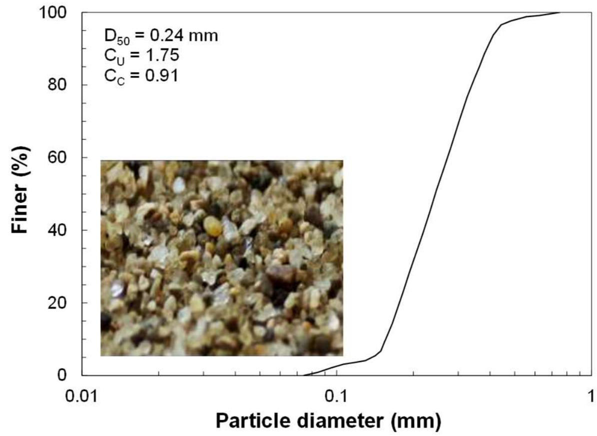

Figure 2. Particle-size distribution and a digital image of Boler sand particles.

2.3 Consolidation and test procedure

Samples were consolidated anisotropically to effective vertical stresses (σ'_{vc}) of 72 to 406 kPa, maintaining a lateral stress coefficient of $K_0 \approx 0.50$ - 0.59. After consolidation, the cone was advanced at a constant rate of 0.42 mm/s into the model sand up to a depth of about 55 mm. Tip (q_c) and sleeve friction (f_s) resistances were logged continuously. One of the CPT tests on a dense sample was also repeated to verify the reproducibility of the CPT resistances.

2.4 Scale and boundary effects

Although miniature calibration chamber testing introduces potential scaling and boundary effects, these were minimized in the present study by adopting a relatively large chamber-to-cone diameter ratio ($D_c/d_c \approx 23$) and penetration depths small relative to specimen dimensions. Previous investigations (Damavandi-Monfared and Sadrekarimi, 2015; Sadrekarimi and Jones, 2022) using the same apparatus demonstrated that cone resistances measured with the miniature cone compare well with results from larger calibration chambers when normalized appropriately, indicating that scale effects are limited within the tested density range. In addition, the maximum D_{rc} in this study was intentionally restricted to moderate values to reduce boundary influence during penetration. Further details on scaling considerations and validation of the MCPT system are provided in Damavandi-Monfared and Sadrekarimi (2015) and Sadrekarimi and Jones (2022).

3 EXPERIMENTAL PROGRAM

A total of 13 MCPTs were conducted across three relative densities and four stress levels. The test matrix is summarised in Table 1.

Table 1. Summary of MCPTs carried out in this study.

Test No.	D_{rc} (%)	σ'_{vc} (kPa)	K_0
CPT-25-1	24	72	0.51
CPT-25-2	28	108	0.52
CPT-25-3	28	204	0.51
CPT-25-4	29	405	0.51
CPT-45-1	45	76	0.52
CPT-45-2	47	101	0.51
CPT-45-3	47	203	0.56
CPT-45-4	48	406	0.59
CPT-65-1	64	76	0.54
CPT-65-2	62	103	0.56
CPT-65-3	65	201	0.50
CPT-65-4	67	402	0.51
CPT-65-4R	66	405	0.52

4 RESULTS

4.1 Representative q_c and f_s profiles

Figure 3 presents typical q_c and f_s profiles in loose, medium-dense, and dense specimens for different σ'_{vc}. Both parameters increased systematically with density and σ'_{vc}. Near-surface q_c rose steeply due to the rapid mobilization of soil resistance, stabilising after 20 - 30 mm of cone penetration. Friction ratios (f_s/q_c) ranged between 0.6% and 1.2%, consistent with drained silica sands. The somewhat larger variability and different CPT resistance trends of test CPT-25-2 were likely due to minor specimen non-uniformity associated with air pluviation, which can lead to localized density variations in loose sand specimens. Nevertheless, the ultimate q_c and f_s measured after approximately 40 mm penetration were consistent with those obtained in the other CPT-25 tests conducted at similar densities. The average q_c and f_s values measured after 40 mm of penetration in each test were subsequently used in developing engineering correlations and data analysis.

As further shown in Figure 3(c), the repeated test CPT-65-4R produced very similar q_c and f_s profiles to those of the original test CPT-65-4, particularly in the steady penetration region beyond approximately 40 mm depth, indicating good repeatability of the MCPT measurements. Because the repeated and the original tests yielded nearly identical ultimate q_c and f_s values, the results from the original test are subsequently used in the analyses and interpretations presented in this study.

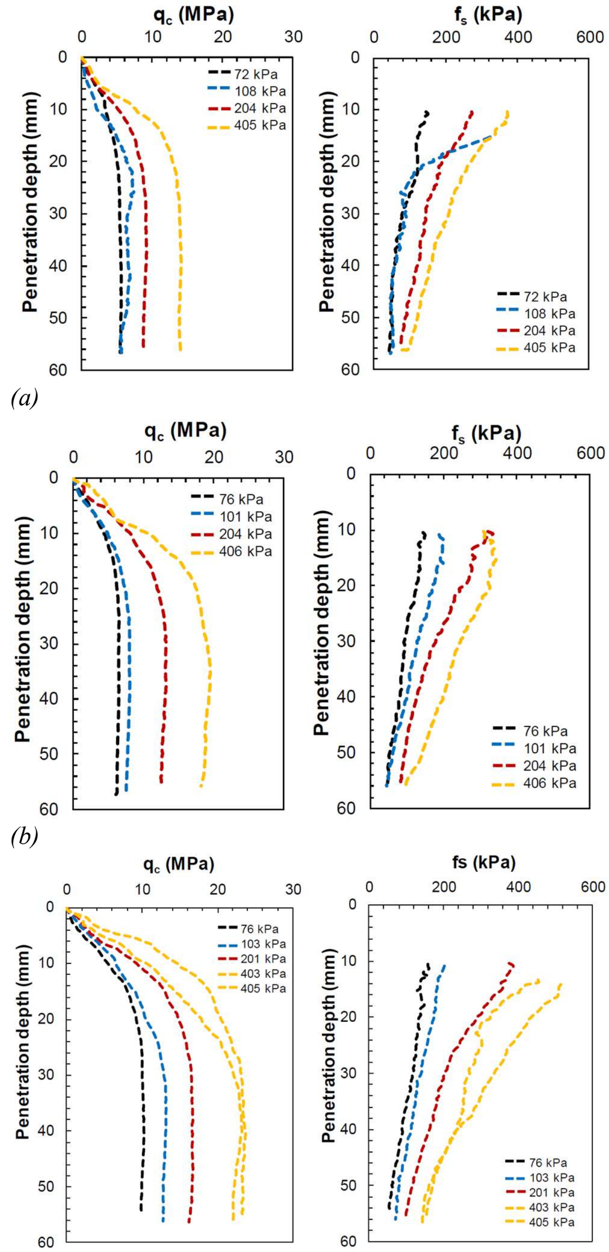

(c)

Figure 3. Typical q_c and f_s profiles in (a) loose (D_{rc} = 27%), (b) medium-dense (D_{rc} = 47%), and (c) dense (D_{rc} = 65%) models.

4.2 Overburden stress normalisation

The influence of σ'_{vc} on q_c and f_s was accounted for by applying normalization relationships of the form:

$$q_{c1} = q_c \left(\frac{P_a}{\sigma'_{vc}}\right)^n \quad (1)$$

$$f_{s1} = f_s \left(\frac{P_a}{\sigma'_{vc}}\right)^c \quad (2)$$

where P_a is the atmospheric pressure (= 100 kPa), σ'_{vc} is the overburden pressure in kPa, and q_{c1} and f_{s1} are overbuden stress-normalized q_c and f_s, respectively. The exponents n and c reflect the degree of stress dependency of the measured responses.

As illustrated in Figures 4 and 5, the normalized cone resistance (q_{c1}/q_c) and sleeve friction (f_{s1}/f_s) data converge toward nearly unique relationships irrespective of confining stress. Based on regression of the presented test data, n was found to range between approximately 0.47 and 0.65, while c varied between 0.52 and 0.56, depending on the relative density of the sand. These values fall well within the range reported in the literature for silica sands, indicating that the stress normalization approach effectively compensates for overburden effects. It is also noted that the medium-density tests ($D_{rc} \approx$ 45 - 48%) exhibited slightly lower q_{c1}/q_c compared with both the loose and the dense specimens. This behaviour is attributed to differences in specimen fabric development and consolidation response at intermediate D_{rc}, where partial collapse of the initially pluviated structure and localized density variations can influence penetration resistance. Because cone resistance is highly sensitive to local packing and stress history, small variations in fabric at intermediate densities may produce apparent deviations in normalized ratios without indicating systematic error. The results are nevertheless consistent with established empirical correlations derived from past chamber and field studies, including those proposed by Liao and Whitman (1986), Kayen et al. (1992), Moss et al. (2006), and Olsen and Mitchell (1995). These reference relationships were developed from generalized databases comprising sands from multiple laboratory and field sites rather than a single calibration material. The soils included in these studies covered a broad range of particle sizes, typically with $D_{50} \approx$ 0.08 - 0.70 mm, encompassing both clean and silty sands with varying depositional histories and aging conditions. For example, Olsen and Mitchell (1995) incorporated calibration chamber results obtained on Monterey sand ($D_{50} \approx$ 0.45 - 0.50 mm) together with field measurements from other sands. In comparison, the Boler sand used in this study is somewhat finer (D_{50} = 0.24 mm) but falls well within the range of materials represented in these databases. Therefore, the comparisons presented here demonstrate agreement with the overall stress-normalization behaviour of sands rather than correspondence with a specific soil type. The close alignment between the present data and the published trends indicates that the selected stress exponents adequately capture the stress dependency of both q_c and f_s, and confirms that the MCPT system can provide reliable measurements comparable to standard-scale tests when appropriate normalization procedures are applied.

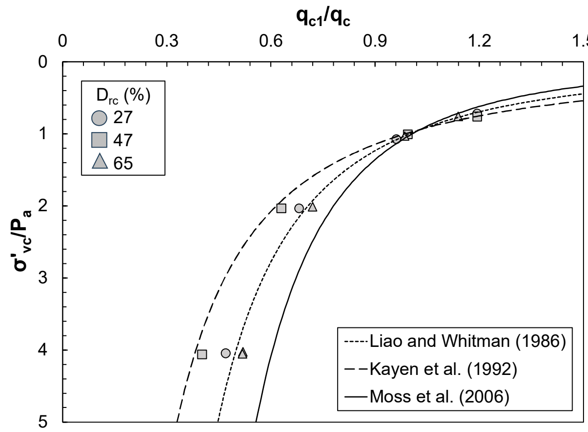

Figure 4. Normalisation of cone tip resistance (q_{c1}/q_c) from the MCPT of this study and comparisons with those proposed by previous studies.

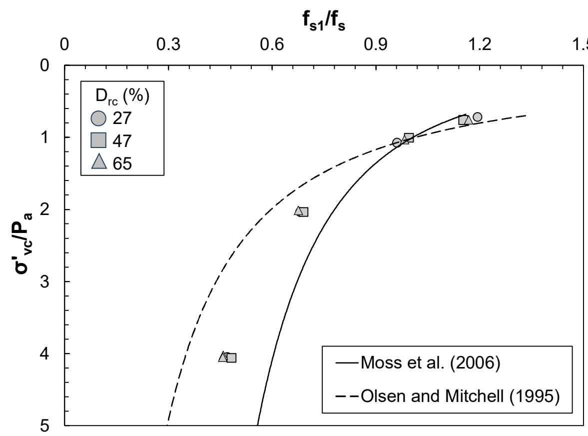

(b)

Figure 5. Normalization of sleeve friction resistance (f_{s1}/f_s) from the MCPT of this study and comparisons with those proposed by previous studies.

4.3 Correlations with unit weight

Empirical relationships were established between the dimensionless normalized parameters $q_{c1N} = q_{c1}/P_a$ and $f_{s1N} = f_{s1}/P_a$ and the Boler sand's dry (γ_{dry}) and saturated (γ_{sat}) unit weights, as illustrated in Figures 6 and 7. These relationships demonstrate a clear and consistent increase in both normalized cone resistance and sleeve friction with increasing unit weight, reflecting the strong dependence of penetration resistance on sand density and associated fabric stiffness. The obtained regression trends closely follow the following semi-logarithmic relationships with q_{c1N}:

$$\gamma_{sat} = 0.9\ln(q_{c1N}) + 15.5 \quad (3)$$

$$\gamma_{dry} = 1.4\ln(q_{c1N}) + 9.0 \quad (4)$$

And the following linear relations with f_{s1N}:

$$\gamma_{sat} = 1.6 f_{s1N} + 18.0 \quad (5)$$

$$\gamma_{dry} = 2.5 f_{s1N} + 13.1 \quad (6)$$

In all the above relationships, γ_{sat} and γ_{dry} are in kN/m^3. According to Figures 6 and 7, the normalized MCPT data for different D_{rc} clustered along nearly unique curves, indicating that the MCPT setup can accurately capture density-controlled variations in penetration response. The strong semi-logarithmic and linear relationships with respectively q_{c1N} and f_{s1N}, and high coefficients of determination ($R^2 > 0.9$) support the robustness of these correlations for characterizing fine to medium-grained silica sands.

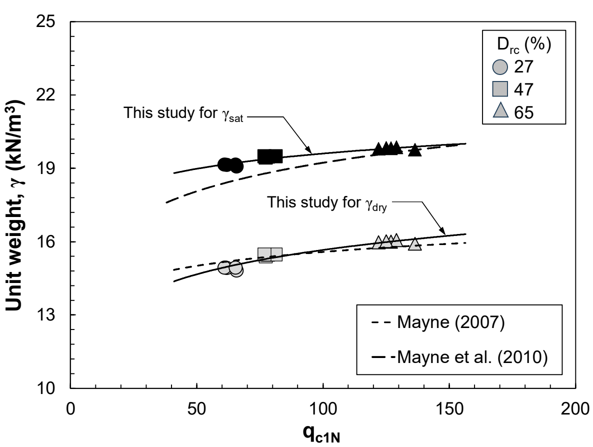

Figure 6. Correlations between γ_{sat} and γ_d with q_{c1N}.

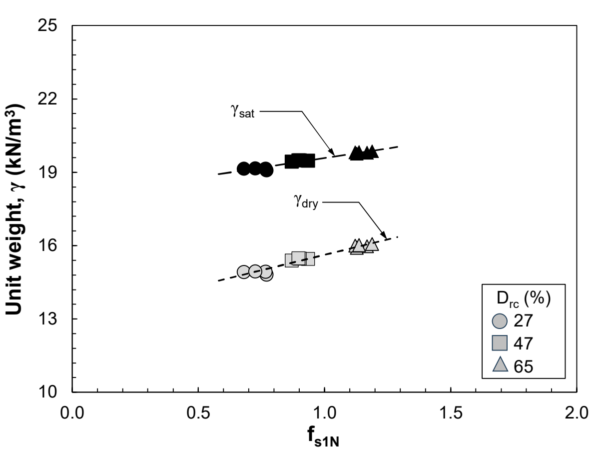

Figure 7. Correlations between γ_{sat} and γ_d with f_{s1N}.

As further demonstrated in Figure 6, the MCPT data of this study and the established trends are very close to those proposed by Mayne et al. (2010) and Mayne (2007) for γ_{sat} and γ_{dry}, respectively. These relationships were developed from extensive CPT databases covering a wide range of sands and sand-like soils obtained from multiple laboratory and field sites. The soils represented in these databases include clean sands, silty sands, hydraulic fills, and natural deposits formed under fluvial, marine, and aeolian conditions, spanning a broad range of particle sizes with typical $D_{50} \approx 0.1$–1.0 mm or larger. The close agreement observed between the present MCPT data and the generalized relationships of Mayne (2007) and Mayne et al. (2010) therefore provides further confirmation that the MCPT can provide a reliable index for estimating the in-situ unit weight of silica sands based on normalized cone and sleeve resistances, offering a valuable tool for developing empirical engineering relationships when large-scale testing is not feasible.

4.4 Correlations with relative density

Figure 8 illustrates a semi-logarithmic relationship established between q_{c1N} and D_{rc} for Boler sand. The data exhibit a strong positive correlation, where q_{c1N} increases exponentially with D_{rc}, reflecting the pronounced influence of soil densification on penetration resistance. The best-fit relationship derived below from this study lies almost entirely within the envelope of the empirical correlation proposed by Villet and Mitchell (1981) based on calibration chamber tests on Monterey No. 0 sand, a uniform subrounded quartz sand with $D_{50} \approx 0.45$ - 0.50 mm, indicating the consistency of the miniature CPT (MCPT) data with large-scale calibration chamber and in-situ test results on clean silica sands.

$$D_{rc}(\%) = 49.5\ln(q_{c1N}) - 174.2 \quad (7)$$

In contrast, other widely used empirical relationships (Jamiolkowski et al., 2001; Baldi et al., 1986; Schmertmann, 1978; Fioravante et al., 1991; Kulhawy and Mayne, 1990) systematically overestimate the relative density of Boler sand, particularly in the loose state ($q_{c1N} < 90$). The correlations of Baldi et al. (1986), Fioravante et al. (1991), and the synthesis presented by Jamiolkowski et al. (2001) were primarily based on Ticino sand, which is a slightly coarser rounded quartz sand with $D_{50} \approx 0.60$ - 0.70 mm. Schmertmann (1978) and Kulhawy and Mayne (1990) compiled relationships from multiple natural deposits with varying mineralogy, grading, and aging effects. In contrast, the Boler sand used in this study is finer (D_{50} = 0.24 mm) and exhibits subrounded to subangular particle morphology. Differences in particle size, angularity, compressibility, and depositional history are known to significantly influence penetration resistance, and therefore some deviation between the present results and previously published correlations is expected.

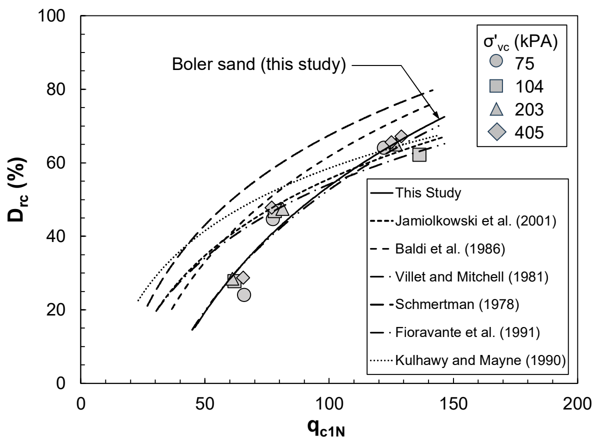

Figure 8. Changes of D_{rc} with q_{c1N} based on the MCPT tests of this study and comparison with those proposed by other studies (Jamiolkowski et al. 2001; Baldi et al. 1986; Villet and Mitchell, 1981; Schmertmann, 1978; Fiorvante et al. 1991; Kulhawy and Mayne, 1990).

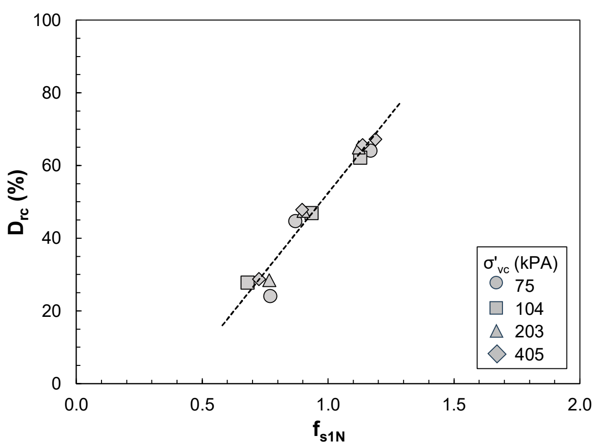

Figure 9. Changes of D_{rc} with f_{s1N} from the MCPT tests of this study.

Figure 9 presents a similar trend between normalized non-dimensional sleeve friction f_{s1N} and D_{rc}, described by the following linear relationship:

$$D_{rc}(\%) = 86.7 f_{s1N} - 34.3 \quad (8)$$

The close alignment and low scatter of the data confirm that sleeve friction readings are also sensitive to density variations and can serve as a complementary index for evaluating D_{rc} in fine to medium sands. Together, these correlations demonstrate the capability of the MCPT system to reliably quantify density-dependent penetration response. Moreover, the results suggest that conventional correlations derived from standard-scale CPTs can be successfully extended to miniature testing when appropriate stress normalization is applied.

4.5 Correlations with constrained modulus

Constrained modulus (M_D) was calculated from each MCPT loading stage based on the slope of the effective vertical stress–axial strain response during one-dimensional consolidation, representing the intermediate-strain stiffness of Boler sand. Figures 10 and 11 plot the resulting values against non-dimensional cone resistances, q_{cN} and f_{sN}, revealing clear and systematic trends between penetration resistance and constrained modulus. The following empirical correlations were established for Boler sand:

$$M_D = 0.23 q_{cN} \quad (9)$$

$$M_D = 7.06 \exp(1.07 f_{sN}) \quad (10)$$

The first expression indicates a linear increase of M_D (in MPa) with increasing q_{cN}, consistent with previously reported relationships (Veismanis 1974; Chapman and Donald 1981; Robertson and Campanella, 1983) for clean silica sands in calibration chamber testing, where stiffness scales directly with normalized cone penetration resistance. The second exponential relationship demonstrates that M_D also grows rapidly with increasing f_{sN}, reflecting the sensitivity of both axial stiffness and shear resistance to densification and fabric interlocking of granular soils.

These correlations confirm that MCPT-derived q_{cN} and f_{sN} readings can be reliably used to estimate constrained modulus in cohesionless soils. In practical terms, this enables direct evaluation of M_D for Boler sand from CPT-based parameters without requiring laboratory consolidation testing, offering a significant advantage for routine geotechnical characterization. Constrained modulus is a critical design parameter governing settlement behavior under drained loading, particularly for shallow foundations, embankments, and backfill performance assessments. Therefore, the strong correlation between M_D and CPT indices developed in this study supports the use of MCPT systems as an efficient tool to obtain stiffness parameters needed for settlement analysis, modulus-based ground models, and deformation-based foundation design.

Furthermore, the consistency and physically meaningful trends in these results highlight that the MCPT apparatus can capture realistic stiffness behavior comparable to standard in-situ testing methods. This reinforces the broader applicability of MCPT for characterizing deformation properties of granular soils in research where field CPT access or sample retrieval may be limited.

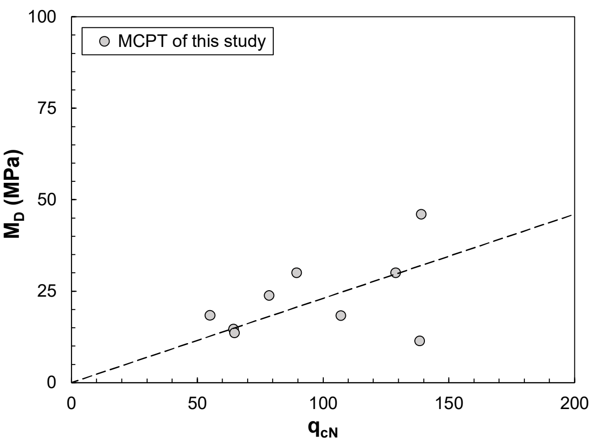

Figure 10. Variation of M_D with q_{cN} based on the MCPT tests of this study.

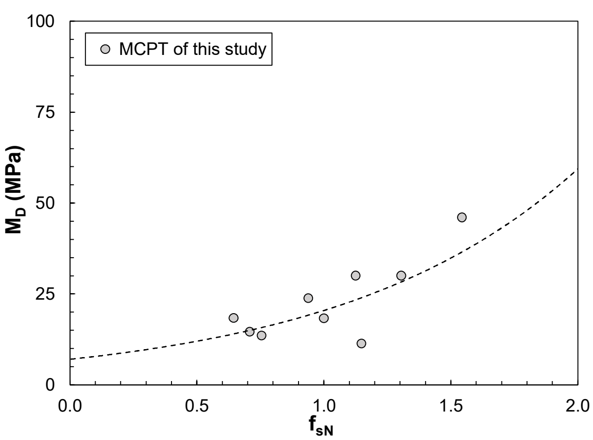

(b)

Figure 11. Variation of M_D with f_{sN} based on the MCPT tests of this study.

5 CONCLUSIONS

The upgraded MCPT system at Western University demonstrated excellent performance in replicating field-consistent penetration behavior of silica sand within a controlled laboratory environment. The system produced repeatable measurements of cone resistance (q_c) and sleeve friction (f_s) across a wide range of effective vertical stresses (σ'_{vc} = 72 - 406 kPa) and relative densities (D_{rc} = 24 – 67%), confirming the reliability and precision of the apparatus for parametric studies. Overburden stress normalization using exponents $n \approx 0.47$ - 0.65 and $c \approx 0.52$ - 0.56 effectively eliminated stress dependency, yielding unified normalized relationships that aligned well with established large-scale CPT results reported in the literature.

The empirical relationships developed between normalized resistances and unit weight revealed strong semi-logarithmic and linear trends, showing excellent agreement with the correlations proposed by Mayne (2007) and Mayne et al. (2010). These findings confirm that normalized MCPT data can be used to accurately estimate both dry and saturated unit weights of silica sands, demonstrating the MCPT's capability to capture density-controlled variations in penetration response. Similarly, a logarithmic relationship was identified between normalized cone resistance and relative density, in close agreement with the Villet and Mitchell (1981) model, while normalized sleeve friction exhibited a strong linear dependence on D_{rc}. Together, these results emphasize that the MCPT effectively captures the influence of soil density and fabric on cone and sleeve resistances, producing data consistent with field-scale penetration behavior.

The correlations established between the constrained modulus (M_D) and normalized cone and sleeve resistances also provide practical value for engineering applications. The observed linear and exponential trends enable reliable estimation of stiffness parameters directly from CPT data, supporting deformation-based foundation design and settlement prediction without the need for extensive laboratory consolidation testing. The consistency and physical relevance of these results demonstrate that the MCPT can reproduce realistic stiffness characteristics comparable to full-scale in-situ CPTs.

Overall, the upgraded MCPT system offers a cost-effective, scalable, and precise platform for studying stress- and density-dependent soil behavior. It provides a robust experimental foundation for developing and refining empirical relationships that link penetration resistance to key geotechnical parameters, bridging the gap between laboratory calibration and field performance.

6 ACKNOWLEDGEMENTS

The authors gratefully acknowledge the assistance of Western University's geotechnical laboratory staff and the foundational work of previous contributors

(including S. Damavandi-Monfared and S. Jones) to the MCPT apparatus development.

7 REFERENCES

ASTM. (2010). Standard D6913: Standard Test Methods for Particle-Size Distribution (Gradation) of Soils Using Sieve Analysis. *In Annual Book of ASTM Standards*. ASTM International, West Conshohocken, PA. p. 34.

ASTM. (2016a). Standard D4254: Standard test methods for minimum index density and unit weight of soils and calculation of relative density. *In Annual Book of ASTM Standards*. ASTM International, West Conshohocken, PA.

ASTM. (2016b). Standard D4253: Standard test methods for maximum index density and unit weight of soils using a vibratory table. *In Annual Book of ASTM Standards*. ASTM International, West Conshohocken, PA.

ASTM. (2014). Standard D854: Standard Test Methods for Specific Gravity of Soil Solids by Water Pycnometer. *In Annual Book of ASTM Standards*. ASTM International, West Conshohocken, PA.

Baldi, G., Bellotti, R., Ghiona, V., Jamiolkowski, M., and Pasqualini, E. (1986). Interpretation of CPTs and CPTUs. Part II: drained penetration of sands. *In Fourth International Geotechnical Seminar on Field Instrumentation and in situ Measurements*, Nanyang Technological Institute, Singapore. pp. 143 - 156.

Chapman, G. A., and Donald, I. B. (1981). Interpretation of static penetration tests in sand. *In 10th International Conference on Soil Mechanics and Foundation Engineering*. Stockholm, A. A. Balkema, Rotterdam, The Netherlands. pp. 455 - 458.

Damavandi-Monfared, S.,and Sadrekarimi, A. (2015). Inte rnal load-cell miniature CPT in a calibration chamber. *Geotechnical Testing Journal*, 38(6), 878–892. https://doi.org/10.1520/GTJ20150036

Fioravante, V., Jamiolkowski, M., Tanizawa, F., and Tatsuoka, F. (1991). Results of CPT's in Toyoura quartz sand. *In 1st International Symposium on Calibration Chamber Testing*, Potsdam, New York. pp. 135 - 146.

Ganguly, R. (2019). *Miniature Cone Penetration Tests with Shear Wave Velocity and Electrical Resistivity Measurements in Characterization of Silica Sand*. Department of Civil and Environmental Engineering, Western University, London, Ontario.

Jamiolkowski, M., Lancellotta, R., and Lo Presti, D. (2001). Remarks on the stiffness of sands. *In Pre-failure Deformation of Geomaterials*, 38 3–387.

Kayen, R.E., Mitchell, J.K., Seed, R.B., Lodge, A., Nishio, S., and Coutinho, R. (1992). Evaluation of SPT-, CPT-, and shear wavebased methods for liquefaction potential assessments using Loma Prieta data. In *4th Japan–U.S. Workshop on Earthquake Resistant Design of Lifeline Facilities and Countermeasures for Soil Liquefaction*. Honolulu, Hawaii, pp. 177–192

Kulhawy, F.H., and Mayne, P.H. (1990). *Manual on estimating soil properties for foundation design*. Electric Power Research Institute (EPRI) Report EL-6800, Palo Alto, California.

Liao, S.S.C., and Whitman, R.V. (1986). Overburden correction factors for SPT in sand. *Journal of Geotechnical Engineering*, 112(3): 373-377. https://doi.org/10.1061/(ASCE)0733-9410(1986)112:3(373)

Mayne, P. W. (2007). *NCHRP Synthesis 368: Cone Penetr ation Testing*. Transportation Research Board.

Mayne, P.W., Peuchen, J., and Bouwmeester, D. (2010). Soil unit weight estimation from CPTs. *In 2nd International Symposium on Cone Penetration Testing*, Huntington Beach, California.

Moss, R.E.S., Seed, R.B., and Olsen, R.S. (2006). Normalizing the CPT for overburden stress. *Journal of Geotechnical and Geoenvironmental Engineering*, 132(3): 378-387. https://doi.org/10.1061/(ASCE)1090-0241(2006)132:3(378)

Olsen, R.S., and Mitchell, J.K. (1995). CPT stress normalization and prediction of soil classification. In *International Symposium On Cone Penetration Testing, CPT'95*. Linkoping, Sweeden, pp. 257 - 262.

Robertson, P. K., and Campanella, R. G. (1983). Interpreta tion of cone penetration tests. *Canadian Geotechnical Journal*, 20(4), 718–733. https://doi.org/10.1139/t83-078

Sadrekarimi, A., and Jones, S. (2022). Laboratory-scale seismic CPT calibration chamber tests on Fraser River sand. *Canadian Geotechnical Journal*, 59(8). https://doi.org/10.1139/cgj-2020-0775

Schmertmann, J. (1978). *Guidelines for Cone Penetration Test: Performance and Design*. FHWA, U.S. DOT.

Veismanis, A. (1974). Laboratory investigation of electrical friction - cone penetrometers in sand. *In European Symposium on Penetration Testing*, Stockholm, pp. 407 - 420.

Villet, W. C. B., and Mitchell, J. K. (1981). Cone resistance, realtive density, and friction angle. In *Proc. ASCE Symp. on Cone Penetration Testing and Experience*. New York, American Society of Civil Engineers, pp. 178 - 208.